

CHAPTER 180

Numerical simulation of sand in plunging breakers

C. PEDERSEN¹, R. DEIGAARD², J. FREDSSØE³ AND E.A. HANSEN⁴

ABSTRACT

A discrete vortex model has been applied to describe plunging breakers. The wave breaking is represented by a jet of water impinging on the surface in front of the wave crest. The suspension of sediment has been modelled by a mixed diffusion - convection scheme. Preliminary results in the form of vector plots of the flow field and concentration profiles are presented.

INTRODUCTION

The surf zone is important for the coastal sediment transport due to the intense production of turbulence and vorticity associated with the wave breaking.

The surf zone is traditionally divided into two regions (Svendsen et al. 1978), the outer surf zone and the inner surf zone. This differentiation is in particular important for the plunging breaking case, where the flow structures in the two regions

¹Ph.D.-student, Institute of Hydrodynamics and Hydraulic Engineering (ISVA), Technical University of Denmark, DK-2800 Lyngby, Denmark.

²Associate Professor, ISVA.

³Professor, ISVA.

⁴Senior research engineer, Danish Hydraulic Institute (DHI), Agern Allé 5, DK-2970 Hørsholm, Denmark

deviate distinctively. In the outer surf zone, the first often violent transformation of the waves takes place. The wave height is reduced rapidly, and the corresponding loss in wave energy is transformed partly into small scale turbulence and partly into kinetic energy in a series of coherent large scale eddy structures, which can stretch over the entire local water depth (see eg. Miller, 1976). In the inner surf zone, the first violent transformation has ceased and the waves migrate towards the shore as turbulent bores. Due to its complex structure, modelling of the flow in the outer surf zone is scarce.

The shoaling process and the transformation of a wave until the initiation of breaking can be described by potential flow theory, and potential flow models are able to represent a plunging breaker until the time when the forward moving jet touches the water surface in front of the wave crest, fig. 1, (Longuet Higgins & Cokelet, 1976).

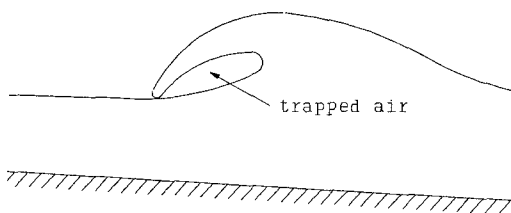


Fig. 1 Jet impingement in plunging breaking wave.

Outside the surf zone the turbulence is mainly generated in the near-bed boundary layer and the sediment transport can be described by the turbulent diffusion equation in connection with a model for the combined wave-current boundary layer, (Fredsoe et al. 1985).

In the inner surf zone, the bore-like broken waves generate turbulence and vortices. The variation in time and space of the turbulence and the suspended sediment can with some accuracy be described by a turbulence model which is coupled with a boundary layer model and the turbulent diffusion equation for the suspended sediment, (Deigaard et al 1986).

The present work is dealing with the situation when the breaking wave plunges, i.e. from the moment when the description by the potential theory breaks down and before the quasi-steady bore approach has become valid. Two mechanisms are dominant for the production of turbulence and vortices.

- The flow pattern generated by the jet impingement on the surface in front of the wave crest, see fig. 2.
- The topologically generated vorticity, see fig. 3. At the instant the jet impinges on the water surface, the domain occupied by the fluid in a vertical section changes from being simply connected to being doubly connected. There is a circulation around the water enclosed core, leading to the formation of a vortex, (Battjes 1988).

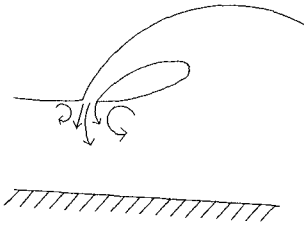


Fig. 2 Vorticity generated by impinging jet.

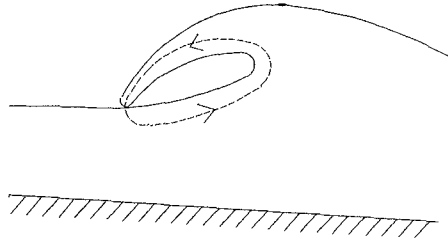


Fig. 3 "Topologically generated" vortex.

The mathematical model will concentrate on the first mechanism, describing the effects from the impinging jet.

THE HYDRODYNAMIC MODEL

General

Despite a large interest in the plunging breaking process over the recent years, the consequent extensive experimental examinations of the mechanisms involved have not yet provided a generally accepted model for the physical process. There are numerous suggestions to how the flow-field develops from the moment of impingement by the jet on the surface, ranging from complete deflection to total penetration of the jet, (Peregrine 1983). The entrainment in- and subsequent escape of air from the water column is accentuated as a main cause for turbulent mixing by some authors, while it is considered insignificant to the flow structure by others.

The varying opinions may partly be due to the complexity of the flow and the accompanying difficulties in performing experimental investigations, but may also result from the fact, that the regime of breaker types are of a more continuous than discrete character. Plunging breaking ranges from the transition from spilling breaking to the transition to surging breaking, (Galvin 1968), spanning over large differences in the magnitudes of the processes involved.

The present study is based on a "well developed" plunging breaking wave, where the jet is assumed to penetrate the water surface in front of the crest as found by Jansen (1986). Effects from the entrainment of air include variable density, buoyancy and compressibility of the fluid. This might be of considerable importance close to the surface, but towards the bottom, the influence is assumed to be less pronounced, and as a first approach it will be neglected, assuming the density of the fluid to be uniform throughout the domain.

The formation of large-scale vortices - "breaker vortices" is generally emphasized as one of the most important features in connection with the exchange of momentum and turbulence with the lower part of the water column (see e.g. Miller 1976). This makes the breaker vortices prime factors in the agitation and suspension of sediment. Nadaoka (1989) further points to the existence of "obliquely descending" eddy structures. For simplicity it has been chosen to treat the problem two-dimensionally in a vertical plane perpendicular to the incoming wave fronts - neglecting possible three dimensional effects in the long shore direction. The observed flow field in this plane comprises the breaker vortices, which are large scale, coherent, vortical flow structures embedded in a highly turbulent region, and therefore calls for a numerical model capable of providing a fine spatial resolution.

Discrete vortex model

The discrete vortex model (DVM) directly simulates the distribution of rotation in the fluid by modelling the rotation as "vorticity particles", which for each timestep are assigned convective and diffusive translations in space. This should fulfill the requirement of spatial resolution of the vorticity in the interior of the computational domain. A simple technique based on superposition of a jet on a non-breaking potential-theory wave has been implemented to simulate the free surface. The emphasis is put on the inner flow field composed of the wave orbital motion and the generation of vorticity due to the jet.

The implemented version of the discrete vortex model is largely similar to the one described by Asp Hansen et al. (1992) and will only be described briefly here. An extensive review of vortex methods has been given by Sarpkaya (1988). The boundary conditions at the surface are unique to the present application of the model and will be described in further detail. The governing equations, which are found from the Navier Stokes equations for incompressible flow in two dimensions combined with the continuity equation, are the vorticity transport equation:

$$\frac{d\omega}{dt} = \frac{\partial\omega}{\partial t} + u \frac{\partial\omega}{\partial x} + v \frac{\partial\omega}{\partial y} \quad (1)$$

and the Poisson equation:

$$\nabla^2 \psi = \omega \quad (2)$$

Here u and v are the velocities in x - and y direction respectively, ν is the kinematic viscosity, ω is the vorticity given by:

$$\omega = \frac{\partial u}{\partial y} - \frac{\partial v}{\partial x} \quad (3)$$

and ψ is the stream-function given by:

$$u = \frac{\partial \psi}{\partial y} \quad ; \quad v = -\frac{\partial \psi}{\partial x} \quad (4)$$

The vorticity transport equation consists of a convective and a diffusive part:

$$\frac{\partial \omega_{conv}}{\partial t} = -u \frac{\partial \omega}{\partial x} - v \frac{\partial \omega}{\partial y} \quad (5)$$

$$\frac{\partial \omega_{diff}}{\partial t} = \nu \nabla^2 \omega \quad (6)$$

Numerically, the governing equations are solved by letting discrete vortex particles represent the vorticity. Each particle has a position in the (x,y) plane and a circulation strength Γ . Further, a finite difference grid is introduced and the calculations performed according to the "cloud in cell" method (Christiansen 1973, Stansby & Dixon 1983). This involves redistribution of the rotation, represented by the discrete vortex particles, to the grid, in which a finite difference version of the Poisson equation is solved. This leads to the stream function $\psi(x,y)$ and thereby the velocity in the grid points (equations 4). The velocity at the position of each particle is found from interpolation, and the convective movement of the discrete particles is performed. The diffusion is simulated by ascribing each particle a small displacement obtained through a random walk procedure. The displacements satisfy a Gaussian distribution, as required by equation (6).

Advancing the solution of a given problem with certain boundary conditions one timestep basically involves the following steps:

1. Solve Poisson's equation (gives $\psi(x,y)$)
2. Determine the velocity field from $\psi(x,y)$
3. Apply new rotation (discrete vortices) to satisfy boundary conditions
4. Move the vortices convectively - equation (5), and approximate a solution to the diffusive transport, equation (6), by use of a random walk procedure

This is a combination of a Lagrangian and an Eulerian description. The discrete vortices are tracked and moved in a Lagrangian fashion, while the Poisson equation is solved in an Eulerian mesh, making the method numerically effective. The cloud in cell method is especially beneficial for a large number of vortices, which is

essential to satisfy boundary conditions and resolve the flow accurately.

The model is implemented in a curvilinear grid, which is generated by solving the Laplace equation for a specified flow through the computational domain.

Boundary conditions for stream function

To solve the Poisson equation (2) in a grid, the stream function ψ needs to be specified along all boundaries of the domain. In the curvilinear grid, the bottom is itself a streamline, implying that ψ_{bottom} is constant.

At the surface, the problem of representing a plunging breaking wave in a fixed grid has been approached by splitting the plunger into two parts: An irrotational "basis wave" and a "jet" of water. The two components are calculated separately based on the mean water level and subsequently superimposed in the model, see fig. 5.

The boundary conditions corresponding to the basis wave - a non-breaking progressive wave - are computed by employing an irrotational formulation of the present model, including a linearized free surface, to the domain and then simulate a wave flap at one side. The "free surface" is established on the basis of the kinematic (7) and the dynamic (8) boundary conditions:

$$dy = \frac{\partial \eta}{\partial t} dt + \frac{\partial \eta}{\partial x} dx \tag{7}$$

$$\frac{\partial u}{\partial t} + u \frac{\partial u}{\partial x} + v \frac{\partial u}{\partial y} = -\frac{1}{\rho} \frac{\partial p}{\partial x} \tag{8}$$

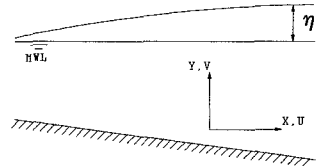


Fig. 4 Definition sketch

Introducing the stream function (4) in the kinematic condition (7) yields:

$$-\frac{\partial \psi}{\partial x} = \frac{\partial \eta}{\partial t} + \frac{\partial \psi}{\partial y} \frac{\partial \eta}{\partial x} \tag{9}$$

Linearizing the dynamic condition (8) eliminates the two convective terms:

$$\frac{\partial u}{\partial t} = -\frac{1}{\rho} \frac{\partial p}{\partial x} \tag{10}$$

Using shallow water theory (hydrostatic pressure distribution) the horizontal pressure gradient is determined by the change in surface elevation:

$$\frac{\partial p}{\partial x} = \rho g \frac{\partial \eta}{\partial x} \quad (11)$$

which introduced in (10) together with the stream function (4) leads to:

$$\frac{\partial}{\partial t} \left(\frac{\partial \Psi}{\partial y} \right) = -g \frac{\partial \eta}{\partial x} \quad (12)$$

Cross differentiating and combining the kinematic and the dynamic conditions yields:

$$\frac{1}{g} \frac{\partial^2}{\partial t^2} \left(\frac{\partial \Psi}{\partial y} \right) = \frac{\partial^2 \Psi}{\partial x^2} \quad (13)$$

which has been integrated over the depth and implemented in a discrete version in the model.

When the boundary conditions (ψ) corresponding to a non-breaking wave have been determined, breaking is simulated by decreasing the wave height from the point of breaking and superimposing a jet on the surface in front of the wave crest. The jet (or pulse) is specified as a vertical velocity component and is moved shoreward with the wave celerity (see fig. 5 & 6). The width, velocity and area of impingement of the jet are specified as functions of time. To satisfy the continuity equation at any time, the water flux introduced in the jet is taken at the crest region, see fig. 5.

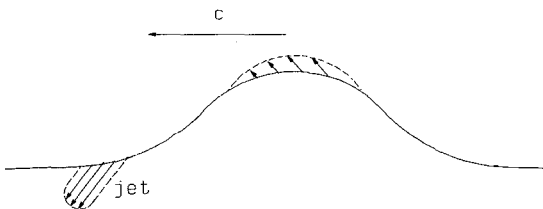


Fig. 5 Velocity components introduced to simulate jet and satisfy continuity.

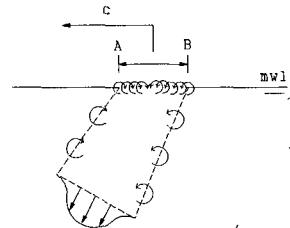


Fig. 6 Vorticity is introduced between A and B.

The sketched method is obviously quite crude, neglecting effects like the entrainment of air and the formation of a turbulent bore. Since the main interest is not the surface features, but rather the convection/diffusion of vorticity into the flow and the eventual effect on the bottom, the technique can serve as a first approach.

Generation of vorticity.

The vorticity can only result from shear layers due to forced velocity gradients at the boundaries. At the bottom, the no slip condition has to be satisfied, while at the surface, the jet is introduced as a velocity field forced upon the initial potential flow field arising from the migrating wave. At the surface, the definition of the vorticity:

$$\omega = \frac{\partial u}{\partial y} - \frac{\partial v}{\partial x} \quad (14)$$

is used to specify the circulation. The horizontal gradient in v has already been specified through ψ , while the vertical gradient in u determines the angle of intrusion of the jet. The flux of vorticity during each timestep is calculated through the information about the production of vorticity and the vertical velocity. It is introduced as discrete particles at the position of the jet (from A to B in fig. 6).

At the bottom, the approach by Asp Hansen et al. (1992) has been implemented. Vorticity is introduced based on a calculation of the flux of vorticity in the boundary layer. The production of vorticity only depends on the velocity U_0 at the outer limit of the boundary layer, while the distribution over the depth depends on the velocity profile and boundary layer thickness. Based on simplifying assumptions (a logarithmic velocity profile in the boundary layer; onset and development of a new boundary layer every time the flow reverses; only slight curvature of the boundary), the boundary layer thickness δ and the friction velocity U_f are found from an approach introduced by Fredsøe (1984) to solve the momentum equation for the boundary layer as derived by Von Kármán:

$$\int_0^{\delta} \rho \frac{\partial u}{\partial t} dy + \frac{\partial}{\partial x} \int_0^{\delta} \rho u^2 dy - u_0 \frac{\partial}{\partial x} \int_0^{\delta} \rho u dy = -\delta \frac{\partial p}{\partial x} - \tau_0 \quad (15)$$

The outer velocity U_0 is as a rough approximation taken at a fixed level above the bottom.

SEDIMENT TRANSPORT

A widely used method to model suspended sediment is by applying a diffusion equation in the vertical direction. This requires knowledge of the vertical distribution of the turbulent quantities of the flow, e.g. represented by the eddy viscosity ν_t , which in the present case has a highly non-uniform character. Close to the plunging point, the convection in the vertical direction due to the large scale vortical structures is expected to be dominant, for which reason the diffusion-model is not feasible.

To take full advantage of the spatial resolution of the flow provided by the discrete vortex model, the sediment is represented by a Lagrangian model when it has been brought away from the bottom. Because it is impossible to trace every single grain, the sediment brought into suspension is modelled as "concentration particles", each representing a certain amount of sediment - much like the case for the discrete vortex particles. In the outer flow, the concentration particles are relocated on a pure convective basis with a fall velocity added. The diffusion due to the small-scale turbulence, which is not resolved in the hydrodynamic model, is assumed negligible compared to the convective transport.

In the near-bed boundary layer the small scales of turbulence are important for the vertical transport of sediment through diffusion. This cannot be resolved by the hydrodynamic model, as it would require a grid with mesh-size in the order of the diameter of the sediment grains. Instead, a boundary layer description based on a diffusion process developed by Asp Hansen et al. (1992) has been employed.

The near-bed concentration of sediment c_b is required as a boundary condition for the diffusion model. The approach by Engelund and Fredsøe (1976), relating the sediment concentration at a distance of twice the grain diameter above the bed to the Shields parameter has been employed. The Shields parameter θ is defined as:

$$\theta = \frac{U_f^2}{(s-1)gd} \quad (16)$$

in which s is the relative density of the sediment, g is the acceleration of gravity, d is the grain size and U_f is the friction velocity obtained from the boundary layer model.

For each timestep the flux of sediment through the level $2d$ is calculated as function of x and introduced in the model as "concentration particles". From the time it is introduced till it settles on the bottom, each particle is tracked in a Lagrangian fashion. In the boundary layer a Monte Carlo simulation is used to simulate the diffusion. This is performed in a similar way as for the vortex particles by use of random displacements following a Gaussian distribution.

RESULTS

The examples of output presented are based on the domain shown in fig. 7. The shoaling waves are propagating from right to left. Breaking is simulated from the point where H/D reaches 0.8, which occurs

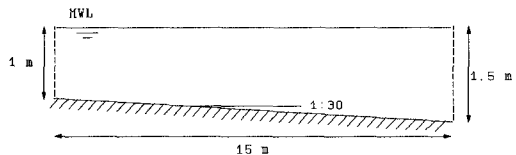


Fig. 7 Model domain

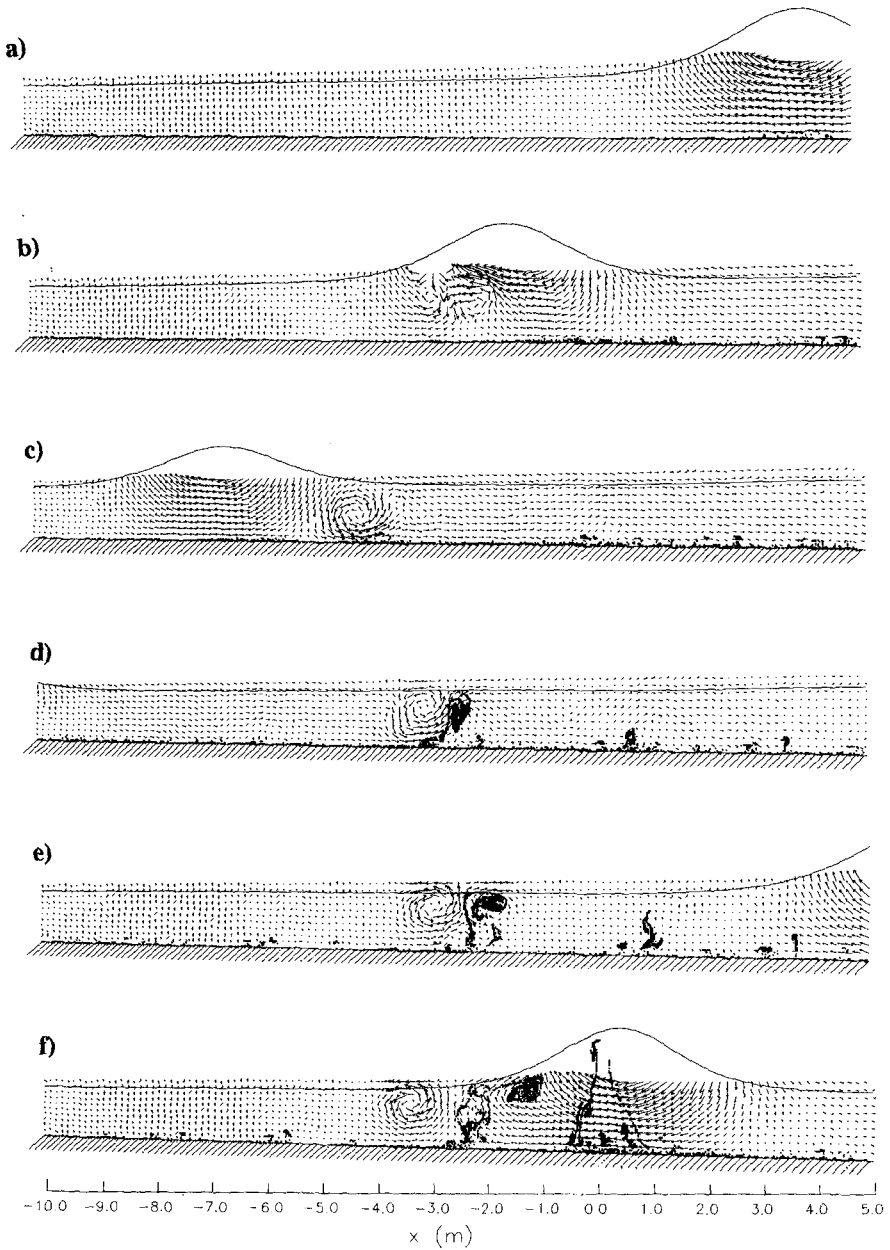
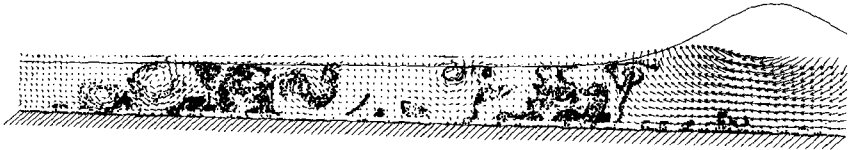


Fig. 8 Vector plot of velocity field from waves migrating through the model domain. The time between each picture is 1.5 s with a wave-period of 6.55. The black dots superimposed on the vector plot represents suspended sediment.

at a water depth of 1.3 m. The wave period is 6.55 sec, the sediment is uniform with a grain size of $d=0.2$ mm., a relative density of $s=2.65$ and a settling velocity of $w_s=0.022$ m/s.

Fig. 8 shows vector plots illustrating the velocity field at various stages. Suspended sediment, represented by concentration particles, is shown as dots. The surface profile represents the wave without the effect from the jet. Picture "a" is a situation before breaking of the first wave, while breaking is occurring in "b". Suspended sediment is still confined to the near-bed region. In "c" one major vortex structure has formed together with weaker disturbances, and in picture "d" these have started convecting sediment into the upper reaches of the flow field. This process develops further in "e" and "f", where the next wave enters the domain.

a)



b)

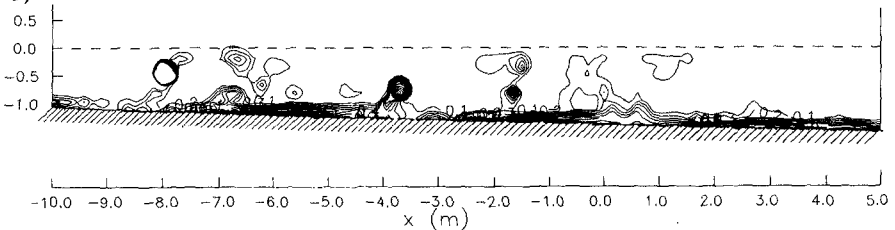


Fig. 9 "Frozen" picture after 10 waves. a) Velocity vectors and particle positions. b) Contours of concentration in the domain.

Fig. 9.a depicts a situation after several waves have passed the area. The suspension of sediment is clearly associated with the large-scale vortex structures in the flow and occurs as plumes of high concentration. This is also seen in fig. 9.b, which shows a contour plot of the concentration at the same moment as 9.a. The plunge point is situated at $x=0$, and the mean water level is at $y=0$. The concentration close to the bottom is not resolved accurately in the plot because of the very high concentrations in the thin boundary layer. The concentration in the plumes reaches values of up to 7 g/l ($\approx 2.6 \cdot 10^{-3}$ m³/m³).

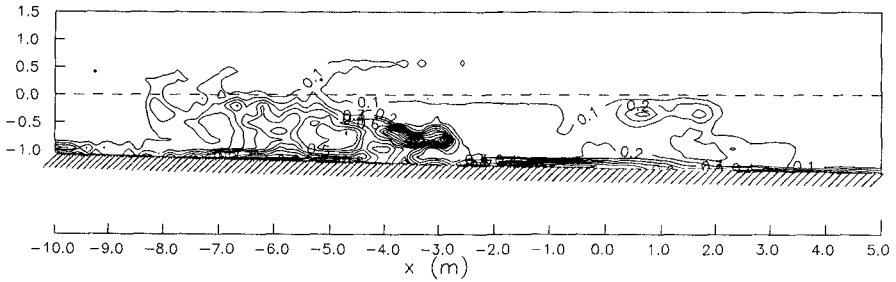


Fig. 10 Concentration averaged over 5 wave periods

Fig. 10 shows a contour plot of the time averaged concentration. The time averaged concentration is highest between 3m and 4m inshore of the plunge point. This coincides with the position where the major vortex formed at breaking reaches the bottom, as seen from fig. 8. The concentration in fig. 10 has been averaged over 5 wave periods after a "quasi-steady" state has been reached with balance between sediment brought into suspension and sediment settling to the bottom. A more uniform distribution could possibly be obtained by averaging over a higher number of periods. The concentration close to the side boundaries of the domain is underestimated because particles are allowed to be convected out of the domain through the boundaries under the influence of the orbital motion of the fluid, while no sediment is reintroduced through the boundaries when the flow is directed into the domain.

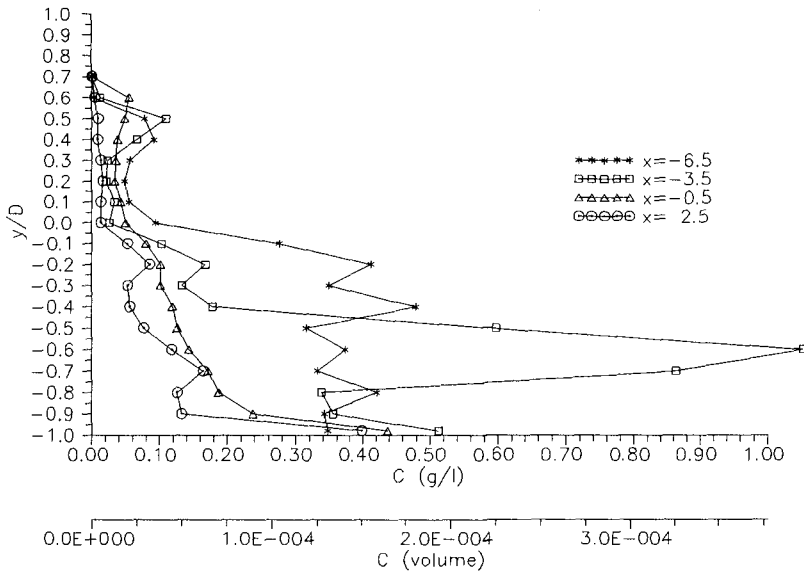


Fig. 11 Time averaged concentration profiles at selected positions relative to the plunge point.

Fig. 11 shows the concentration plotted as function of the dimensionless position above the bottom (y/D) for selected distances relative to the plunge point. The profiles differ distinctively from the "usual" diffusion profile, which can be contributed to the dominating role of convection.

CONCLUSIONS

The discrete vortex model is capable of resolving the major vortex structures of the flow, which by convection brings sediment from the near-bottom region to the upper reaches of the water column. The small-scale turbulence in the boundary layer cannot be resolved by the discrete vortex model, as this would require too fine discretization in space and time. Instead a diffusion model has been used to simulate the suspension of sediment in the boundary layer.

Under the influence of the wave motion and the vortex structures created by the wave breaking, the sediment is convected through the model domain as unevenly distributed plumes. Preliminary results show, that with waves breaking at a water-depth of 1.3 m and sediment represented by a grain size of 0.2 mm., a relative density to water of 2.65 and a settling velocity of 0.022 m/s, the concentration in the plumes may reach values of 7 g/l ($\approx 2.6 \cdot 10^{-3} \text{ m}^3/\text{m}^3$). The time-averaged concentration away from the bottom reaches a value of 1 g/l at a position approximately 2 times the local water depth in-shore of the plunge point, and decreases towards both sides.

ACKNOWLEDGEMENT

This work was undertaken as a part of the MAST G6 Coastal Morphodynamics research programme. It was founded jointly by the Danish Technical Research Council (STVF) under the programme "Marin Teknik" and the Commission of the European Communities, Directorate General for Science, Research and Development, under MAST contract no. 0035-C.

REFERENCES

- Asp Hansen E., J. Fredsøe, R. Deigaard, 1992, "Distribution of suspended sediment over wave-generated ripples", submitted for publication.
- Battjes J.A., 1988, "Surf-zone dynamics", Annual Review of Fluid Mechanics, 1988, Vol. 20, pp. 257-293.
- Christiansen J.P., 1973, "Numerical simulation of hydromechanics by the method of point vortices", Journal of Computer Physics, Vol. 13, pp. 363-379.

Deigaard R., J. Fredsøe, I. Brøker Hedegaard, 1986, "Suspended sediment in the surf zone", *J. of Waterway, Port, Coastal and Ocean Engineering*, ASCE, Vol. 112, No. 1, pp. 115-128.

Engelund F. and J. Fredsøe, 1976, "A sediment transport model for straight alluvial channel", *Nordic Hydrology*, Vol. 7, No. 5, pp. 293-306.

Fredsøe J., 1984, "Turbulent boundary layer in wave and current motion", *J. of Hydraulic Engineering*, ASCE, Vol. 110, No. 8, pp. 1103-1120.

Fredsøe J., O.H. Andersen, S. Silberg, 1985, "Distribution of suspended sediment in large waves", *J. of Waterway, Port, Coastal and Ocean Engineering*, ASCE, Vol. 111, No. 6, pp. 1041-1059.

Galvin C.J., 1968, "Breaker type classification on three laboratory beaches", *Journal of Geophysical Resources*, Vol. 73, pp. 3651-3659.

Jansen P.C.M., 1986, "Laboratory observations of the kinematics in the aerated region of breaking waves", *Coastal Engineering*, Vol. 9, pp. 453-477.

Longuet-Higgins M.S. and E.D. Cokelet, 1976, "The deformation of steep surface waves on water I, a numerical method of computation", *Proc. of the Royal Society, London*, A 350, pp. 1-26.

Miller R.L., 1976, "Role of vortices in surf zone prediction: Sedimentation and wave forces", *Beach and Nearshore Sedimentation*, SEPM Spec. Pub. 23, pp. 92-114.

Nadaoka K., 1989, "Structure of the turbulent flow field under breaking waves in the surf zone", *J. Fluid Mechanics*, Vol. 204, pp. 359-387.

Peregrine D.H., 1983, "Breaking Waves on Beaches", *Annual Review of Fluid Mechanics*, 1983, Vol. 15, pp. 149-178.

Sarpkaya T., 1989, "Computational methods with vortices - the 1988 Freeman Scholar Lecture", *J. of Fluids Engineering*, Vol. 111, pp. 5-52.

Stansby P.K., A.G. Dixon, 1983, "Simulation of flows around cylinders by a Lagrangian vortex scheme", *Appl. Ocean Res.*, Vol. 5, No. 3, pp. 167-178.

Svendsen I.A., P.A. Madsen, J.B. Hansen, 1978, "Wave characteristics in the surf zone", *Proc. 16th conf. on coastal eng.* 1978, pp. 520-539.